Journal of Non-Newtonian Fluid Mechanics, 40 (1991) 281–288
Elsevier Science Publishers B.V., Amsterdam

Mechanics of the "falling plate" extensional rheometer

Robert W.G. Shipman [a], Morton M. Denn [a] and Roland Keunings [b]

[a] *Center for Advanced Materials, Lawrence Berkeley Laboratory and Department of Chemical Engineering, University of California, Berkeley, CA 94720 (USA)*
[b] *Unité de Mecanique Appliquée, Université Catholique de Louvain, 1348 Louvain-la-Neuve (Belgium)*

(Received December 3, 1990)

Abstract

The low-rate falling-plate extensional rheometer experiments by Sridhar and coworkers on a mobile polymer solution were simulated using a free-surface finite-element code which accounts for gravity and surface tension. There is a reverse flow near the plates which is caused by the interaction between gravitational and surface tension forces, causing a delay in the development of the uniform cylindrical column and a difference between the local and imposed extension rates during the early stages of the experiment.

Keywords: extensional flow; polymer solutions; rheometry

1. Introduction

The measurement of extensional stresses in mobile liquids such as dilute and semi-dilute polymer solutions has received considerable attention in this journal [1]. Matta and Tytus [2] have recently proposed the use of a falling-plate device as an extensional rheometer. The concept of using a falling weight as a means of extending a cylindrical filament and measuring extensional properties is not new and was exploited, for example, by Chen et al. [3] with high-viscosity polymer melts. The attractive feature of Matta and Tytus's experiments on low-viscosity solutions is the observation that the fluid column necked rapidly near the upper and lower plates for the polymer solutions and was essentially cylindrical over most of the flow regime. The device and free surface profile is shown schematically in Fig. 1, where the

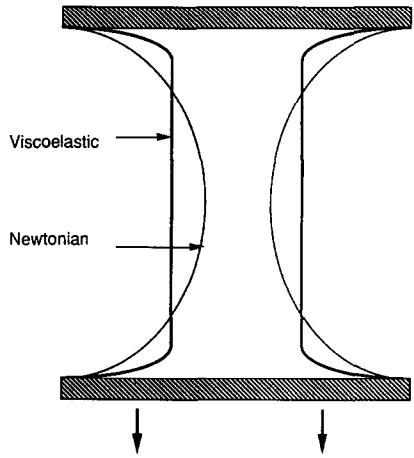

Fig. 1. Schematic of column profiles in the falling-plate extensional rheometer.

figure is drawn to emphasize the more columnar profile observed for the polymer solutions relative to Newtonian test fluids. The geometry thus appears to provide a means of implementing uniform uniaxial extension with low viscosity fluids, a goal which has eluded prior attempts. Sridhar et al. [4] have recently modified Matta and Tytus's design by imposing a fixed exponential rate of separation between the two plates in order to do experiments under constant stretch rate conditions rather than under constant force.

We have simulated the details of one of Sridhar's constant-rate falling-plate rheometer experiments using a transient finite-element method which takes gravity and surface tension into account and uses an Oldroyd-B description of the polymer solution rheology. The Oldroyd-B constitutive equation is a good approximation to the rheology of the fluids studied in both sets of experiments at low and moderate extension rates, but it fails at high rates. All of Sridhar's experiments were carried out at low extension rates (typically less than 1 s^{-1}) and over times greater than ten seconds; we have thus been able to identify the interesting flow characteristics of the experimental system and to obtain some insight into the analysis of data. Matta and Tytus's experiments were carried out at extension rates of more than 10 s^{-1} with typical run times of about 0.1 s, which is on the order of the relaxation time for the polymer solutions used. We were less successful in describing these experiments, probably because the manner in which the boundary conditions are imposed in the simulation is inconsistent with the rapid imposed stretch rate. We have not included simulations of the latter experiments here, but they are recorded in Shipman [5].

2. Simulation

Sridhar's experiments were carried out at room temperature (between 19 and 23°C) with a 1850 ppm solution of polyisobutylene in polybutene. Rheological data are given in [6]; the Oldroyd-B parameters at 20°C, which were used in the simulation, are given in Table 1. The overall extension rate based on plate motion for the simulated run was 0.29 s^{-1}. Diameter profiles as a function of time were measured from photographs provided by Sridhar. The diameter at the thinnest point on the filament is plotted on semi-logarithmic coordinates as a function of time in Fig. 2. There appear to be two regions of constant local extension rate, with a transition occurring at about five seconds; the local and overall extension rates are the same at long times.

The semi-implicit finite element code, which is described elsewhere [7], accounts for variations in the flow domain in the radial direction but requires a fixed axial length. The boundary conditions used were no slip on the plates, symmetry at the center line, no tangential stress on the free surface, and total normal stress balanced by the surface tension stress on the free surface. A stress boundary condition must be imposed at the end of the mesh, and a degree of ambiguity is introduced here. We have chosen to set the normal stress equal to the theoretical steady-state extensional stress of the Oldroyd-B fluid at the imposed overall extension rate. Use of the overall

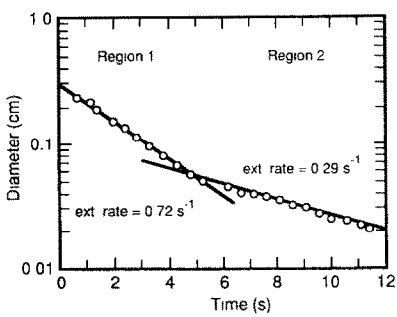

Fig. 2. Filament radius at the thinnest point as a function of time in Sridhar's experiment.

TABLE 1

Oldroyd-B parameters for 1850 ppm solution of polyisobutylene in polybutyene used by Sridhar

η (viscosity)	36.0 Pa. s
η_s (solvent viscosity)	27.0 Pa. s
η_p (polymer viscosity)	9.0 Pa. s
λ_1 (relaxation time)	0.824 s
λ_2 (retardation time)	0.618 s

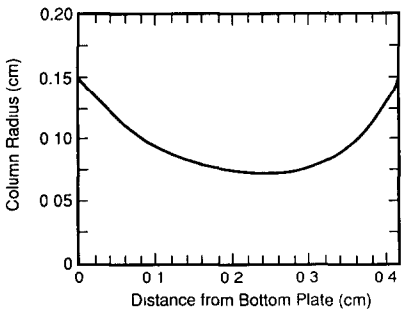

Fig. 3. Free-surface profile at $t = 2.42$ s.

stretch rate and the pseudo-steady-state approximation for stress introduces some error into the simulation, but it is probably acceptable for Sridhar's low-rate experiments. The approximation is clearly not applicable to the short-time experiment of Matta and Tytus.

A second ambiguity is introduced in accounting for the effect of fluid outside the fixed control volume. In Matta and Tytus's free-fall experiment the weight of fluid and disk must be included, but the total weight of fluid is not relevant in the supported column used by Sridhar and coworkers. We have neglected the effect of the fluid head on the pressure in the calculations reported here, since the effect does not appear to be significant when other uncertainties (temperature dependence of fluid properties, for example) are taken into account.

The initial column shape was taken at 2.42 s into the experiment, as shown in Fig. 3. The simulation was not started at $t = 0$ because that would have required too short a mesh to capture the extensional flow in the elongated column at later times. An asymmetry resulting from gravitational forces is to be noted. The initial velocities in the flow domain were taken to be zero since they are unknown; this introduces an error which is expected to be small because of the small effect of inertia after the establishment of flow. Typical finite-element meshes used for the upper and lower portions of the column are shown in Fig. 4. The axial mesh lengths were varied in the calculations to check for sensitivity to the stress boundary condition.

A comparison of the simulated and experimental free-surface profiles at 8.64 s is shown in Fig. 5 using upper and lower meshes of 0.25 and 0.28 cm, respectively. The surface tension was assumed to be 20 dyn cm^{-1}. The agreement is not exact, which is to be expected in view of the uncertainties in both the physical properties and the stress boundary condition, but it is clear that the simulations capture the essential shape of the column at the two plates. Increasing the surface tension to 30 dyn cm^{-1} did not improve the overall fit. Preliminary results accounting for the effect of the fluid head

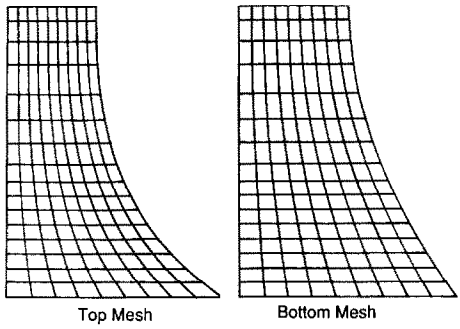

Fig. 4. Top and bottom meshes for simulation of Sridhar's experiment.

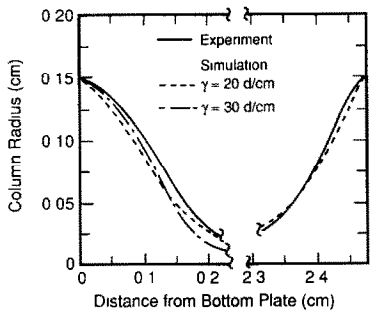

Fig. 5. Comparison of simulation and experimental free-surface profile at $t = 8.64$ s.

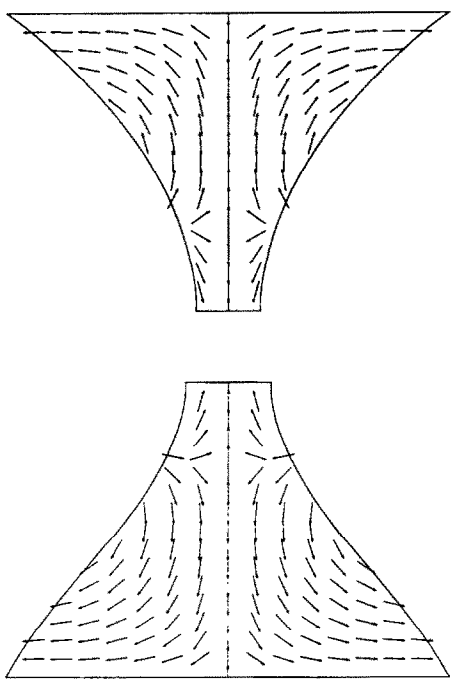

Fig. 6. Flow direction near upper and lower plates.

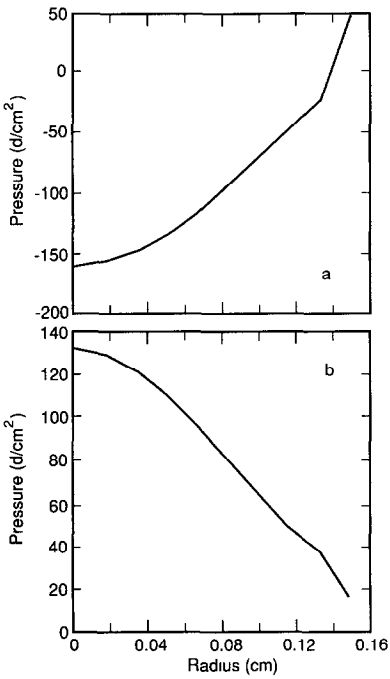

Fig. 7. Pressure profile along top plate: (a) $t = 3.22$ s; (b) $t = 8.82$ s.

outside the control volumes indicated improved agreement but the calculation was not pursued in view of the large number of uncertainties in the simulation. Deviation from a cylindrical shape near the plates is substantial. The flow directions, shown in Fig. 6, are unexpected; there is a significant flow towards the top and bottom plates as well as the expected flow in the direction of extension. (The reference frame for the simulation about the bottom plate is fixed to the accelerating plate; the acceleration is small enough that inertial effects from the accelerating reference frame can be completely ignored.) This reverse flow first appears near the plates and then migrates toward the filament as the filament thins. The phenomenon is accompanied by a change in the pressure gradient along the top plate; the pressure is initially low in the center and high along the edges (Fig. 7a), but becomes high in the center and low along the edges when the reverse flow develops (Fig. 7b).

The free surface shape in the region near the edges of the plates is dominated by the interaction between gravitational and surface tension forces; the pressure differential between the plate and the surface is given by the hydrostatic head of the fluid, and the magnitude of the pressure is determined by the surface tension. The isotropic contribution from surface tension is a major factor in establishing the stress gradient and hence the

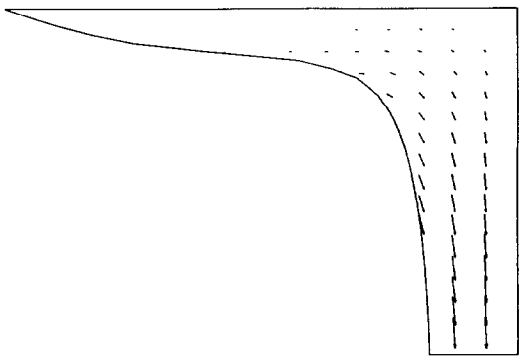

Fig. 8. Flow direction for simulation without surface tension.

shape of the free surface. The capillary pressure for a filament with a radius of 0.05 cm is 400 dyn cm^{-2}, for example, which is comparable to the maximum extensional stresses caused by the stretching flow. A simulation under the same conditions but without surface tension is shown in Fig. 8. There is no reverse flow and the cylindrical section of the column is much longer despite the large difference in radius between the filament and the plate. (The stretching terms are an order of magnitude larger than those due to surface tension in the high-rate viscoelastic experiments of Matta and Tytus, hence the apparent absence of backflow and the rapid establishment of uniform uniaxial stretching.) The development of the reverse flow during the early stage of extension and the concomitant short length of the cylindrical section is the apparent reason for the difference in local extension rates seen in the early and later stages of Sridhar's experiments, where the macroscopic extension rate is observed locally only after the cylindrical column has developed to a sufficient length.

Acknowledgment

This work was supported by the Director, Office of Energy Research, Office of Basic Energy Sciences, Materials Science Division of the U.S. Department of Energy under contract number DE-AC03-76SF00098. We are grateful to Drs. Sridhar and Matta for providing experimental data prior to publication.

References

1 T. Sridhar (Ed.), Proc. Int. Conf. on Extensional Flow, Cambloux, March, 1989, J. Non-Newtonian Fluid Mech., 35 (1990), Nos. 2 and 3.

2 J.E. Matta and R.P. Tytus, J. Non-Newtonian Fluid Mech., 35 (1990) 215.

3 J. Chen, G.E. Hagler, L.E. Abbott, D.C. Bogue and J.L. White, Trans. Soc. Rheol., 16 (1972) 473.
4 T. Sridhar, V. Tirtaatmadja, D.A. Nguyen and R.K. Gupta, J. Non-Newtonian Fluid Mech., 40 (1991) 271.
5 R.W.G. Shipman, Ph.D. Dissertation, University of California at Berkeley, 1990.
6 T. Sridhar, R.K. Gupta, D.V. Boger and R. Binnington, J. Non-Newtonian Fluid Mech., 21 (1986) 115.
7 R. Keunings, J. Comput. Phys., 62 (1986) 199.